UDC 681.586.728 DOI: 10.15222/TKEA2025.3-4.15

Viktor SERGIICHUK, Ostap OLIINYK

Ukraine, Igor Sikorsky Kyiv Polytechnic Institute
E-mail: ostap.oliinyk@gmail.com

DEVELOPMENT OF A MATHEMATICAL MODEL FOR A CdS-BASED PHOTOSENSITIVE HALL SENSOR

The paper proposes a mathematical model of a photosensitive Hall sensor based on a CdS single crystal which uses the internal photoelectric effect. The model describes the change in the concentration and mobility of charge carriers under irradiation and allows estimating the increase in the sensor's sensitivity to a magnetic field. The model accurately describes the increase in Hall voltage when the sensor current exceeds 40 mA (error margin of less than 5%). Experiments showed a 2.8-fold increase in sensor sensitivity in the low-current sensor mode, which is partially due to noise and additional effects in the crystal. The proposed materials and sensor topology can help maximize Hall voltage to obtain maximum sensor sensitivity. The comparison of theoretical results and experimental data confirmed a twofold increase in the Hall voltage under irradiation.

Keywords: Hall effect, photosensitive Hall sensor, CdS, mathematical modeling, planar Hall sensor.

In modern sensor technology, there is a sustained increase in requirements for accuracy, energy efficiency, and functional integration of measurement devices. In particular, in the fields of automotive electronics, biomedical systems, and wireless sensor networks, the demand for multifunctional sensors capable of operating simultaneously based on several physical principles is steadily growing [1], [2]. One of the promising directions is the integration of the Hall effect with the photoelectric effect within a single semiconductor element, which opens up opportunities to enhance magnetic field sensitivity through additional photogeneration of charge carriers.

Conventional Hall sensors are characterized by high reliability and accuracy and are widely used in magnetometry, positioning systems, and current sensing applications [3]. At the same time, their performance remains limited by a constant charge carrier concentration and geometric dimensions, without accounting for temperature effects, magnetic field configuration, carrier concentration fluctuations, and related factors. Recent studies have demonstrated that optical irradiation can significantly alter the electrical conductivity of semiconductors, affecting both the concentration and mobility of charge carriers [4].

In [5], it was demonstrated that directed illumination during Hall measurements opens new possibilities for material diagnostics, including defect spectroscopy, evaluation of photogeneration processes, and assessment of the contributions of electrons and holes along with their mobilities. Hall photoeffect spectroscopy with a controlled radiation flux has shown high sensitivity to recombination centers and even the occurrence of negative differential photoconductivity (**NDPC**) in semiconductors, which is consistent with the concept of an "active layer" and with changes in the concentrations of electrons and holes, as well as their mobilities, under external irradiation.

A useful extension in the context of the present work is the light-modulated Hall effect (**LMHE**) [6]. By introducing optical modulation and employing phase-sensitive detection of the Hall voltage, it becomes possible to separate the photogenerated contribution and to enhance the signal-to-noise ratio in systems with low charge carrier mobility.

Previous studies on the modeling of photoinduced effects in semiconductors [7], [8], [9] have demonstrated the influence of photon flux, quantum efficiency, and charge carrier lifetime on the transport properties of materials. However, most existing models consider static conditions or isolated optical phenomena without comprehensively accounting for their interaction with the classical Hall effect. This creates a scientific niche for the development of a more generalized mathematical model that integrates both effects and enables prediction of changes in sensor sensitivity under illumination.

Despite the existence of studies addressing individual aspects of the photoinduced Hall effect, the majority of research focuses either on spectroscopic diagnostics of materials or on static analysis of the Hall effect without considering the influence of irradiation. At present, there are no models that consistently describe the combined impact of photogeneration, recombination processes, and variations in charge carrier mobility on the Hall voltage in practical structures based on cadmium sulfide (CdS) single crystals. These circumstances motivated the development of the mathematical model proposed in this work, which accounts for the effect of irradiation on the parameters of a Hall sensor.

In this work, CdS single crystals are considered a promising sensing material, as they combine high photoconductivity in the visible spectral range — compared with other materials — with relatively high electron mobility (100 – 600 cm²/(V·s)), low hole mobility (15 – 70 cm²/(V·s)), and *n*-type conductivity, which ensures an increase in the Hall voltage under illumination. The bandgap width is $E_g \approx 2.4$ eV, making CdS particularly effective for photoelectron generation in the visible wavelength range (480 – 550 nm), where maximum photoconductivity and minimal losses due to thermodynamic processes are achieved. In addition, CdS is characterized by a relatively low intrinsic charge carrier concentration in the dark state, which enables clear separation of the photogenerated EMF contribution within the Hall voltage. CdS-based structures are well compatible with planar microfabrication technologies, exhibit stable electrophysical parameters at constant temperature, and provide reproducible results, making this material suitable for the investigation of photosensitive Hall sensors and their subsequent practical implementation.

Theoretical Analysis of the Effect of Optical Irradiation on CdS Parameters and the Hall Voltage

The classical physical model accounting for the topology of a Hall sensor is based on the phenomenon of transverse voltage occurring when current passes through a conductor (or semiconductor) placed in an orthogonal (crossed) magnetic field. This phenomenon, first discovered by Edwin Hall in the late nineteenth century, is widely employed for measuring magnetic flux density and for the indirect determination of a range of other physical quantities [1], [2].

The classical expression for the Hall voltage can be written as

$$U_H = \frac{IB}{ned} = R_H \frac{IB}{d}, \quad (1)$$

where I is current through the sensor;

B is magnetic flux density (magnetic field intensity);

n is charge carrier concentration in the material;

e is elementary charge (electron or hole);

d is thickness of the sensing element along the direction in which the Hall voltage is generated;

R_H is Hall coefficient, $R_H = 1/(ne)$.

The classical Hall sensor model assumes that the semiconductor or metallic plate is homogeneous in thickness and composition, that charge carriers move within it in accordance with Ohm's law under the action of the Lorentz force in a magnetic field, and that edge effects do not have a significant influence and are therefore neglected.

In practice, the shape and dimensions of a sensor may deviate from the idealized model, and the thickness and material properties of the crystal may be non-uniform. This is commonly accounted for by introducing a dimensionless geometrical correction factor G into equation (1):

$$U_H = R_H \frac{IB}{d} G. \quad (2)$$

In more complex systems, it is essential to account for the charge carrier mobility μ and recombination processes. In the case of doped semiconductors, where different types of charge carriers (electrons and holes) coexist, the Hall coefficient is expressed as the combined contribution of each carrier type. Under these conditions, equation (2) takes the form:

$$U_H = \frac{p\mu_h^2 - n\mu_e^2}{q\left(p\mu_h + n\mu_e\right)^2} \frac{IB}{d} G, \quad (3)$$

where μ_h, μ_e is the mobilities of holes and electrons, respectively.

The classical model provides a convenient and efficient means for estimating the key parameters of a Hall sensor, such as sensitivity and output signal, which is particularly useful in the early stages of device design [2]. However, the classical model has certain limitations, as it does not take into consideration temperature effects, magnetic field intensity, or external optical irradiation.

Several models [10], [11], [12] proposed to describe Hall sensors incorporate additional effects or parameters, such as anisotropic conductivity in the semiconductor crystal, surface scattering, and charge carrier transport phenomena. Nevertheless, parameters such as carrier concentration, sensor thickness, and mobility are typically assumed constant, being determined during the design and fabrication stages. Given that these parameters can vary under optical irradiation, it is necessary for the model to account for the internal photoelectric effect and its influence on the Hall voltage.

Over the past two decades, numerous experimental and theoretical studies have investigated the effects of charge carrier photogeneration in semiconductor structures. Photogeneration significantly increases the charge carrier population in a semiconductor, thereby modifying its electrical conductivity [13]. In particular, studies [14], [15] have demonstrated that the contributions of electrons and holes can be accurately separated, and their mobilities can be determined in high-mobility organic semiconductors under optical excitation. Photogeneration has been shown to substantially affect both carrier concentration and effective mobility, which is consistent with the assumptions underlying the present work.

In the context of contactless conductivity measurement techniques, it is also important to note the phenomenon known as the optical hall effect, which enables evaluation of free carrier parameters (concentration, mobility, and effective mass) without direct electrical contact, by employing a magnetic field and an optically excited medium. For example, the authors of [16] presented a

ISSN 3083-6530 (Print)
ISSN 3083-6549 (Online)

detailed model of the optical hall effect dielectric tensor function for multilayer semiconductor structures and explained how data analysis based on Mueller matrices and 4×4 matrix formalisms provide access to the electrical characteristics of the material.

Optical irradiation affects not only carrier concentration but also carrier mobility, both of which are critical for sensor operation. The expression for the change in the excess carrier concentration Δn in a semiconductor under external irradiation is given by:

$$D = \frac{\mathrm{d}n}{\mathrm{d}t} = \frac{\Delta n}{\tau}, \tag{4}$$

where D is charge carrier generation rate;
τ is lifetime of nonequilibrium charge carriers.

The mobility of electrons and holes is determined by the expression:

$$\mu = e\tau / m^*, \tag{5}$$

where m^* is the effective mass of a charge carrier.

From expression (4), the time-dependent change in the concentration of nonequilibrium charge carriers $\Delta n(t)$ relative to the initial (intrinsic) carrier concentration $n(0)$ can be derived [17]:

$$\Delta n(t) = n(0) \cdot \exp(-t/\tau). \tag{6}$$

The photogeneration parameters, in particular the quantum efficiency and the absorption coefficient, determine the magnitude and linearity of the photosensitive signal and can be incorporated into the sensor model. Since the recombination rate is inversely proportional to the carrier lifetime, the quantum efficiency can be expressed as follows:

$$\eta_q = \frac{\tau_{nr}}{\tau_r + \tau_{nr}}, \tag{7}$$

where τ_{nr}, τ_r is carrier lifetimes in the absence of irradiation and under irradiation, respectively.

The amplitude of the output signal is determined by the change in the resistance R of the active region of the sensor and depends on the quantum efficiency η and the absorption coefficient α:

$$R = \eta \frac{e}{h\nu}(1 - \exp(-\alpha d)), \tag{8}$$

where $h\nu$ is the energy of the incident photon.

Photogeneration exhibits pronounced dynamic properties that affect the sensor response time and its frequency characteristics. This implies that models accounting only for the static influence of light may be insufficiently accurate for describing sensor operation under time-varying irradiation conditions [18]. Accordingly, the frequency dependence of the photoinduced current can be expressed as follows:

$$I_{ph}(\omega) = \frac{D_0 \mu E}{1 + (\omega\tau)^2}, \tag{9}$$

where D_0 is amplitude of the charge carrier generation rate;
E is the electric field;
ω is the angular modulation frequency.

Despite significant progress in understanding photogeneration in semiconductors, several key aspects remain insufficiently studied or generalized in contemporary models, such as the nonlinear interaction between photogeneration and the classical Hall effect [19], [20] dynamic variations of photogeneration and their impact on the temporal characteristics of sensors [21], [22], as well as the interplay between optical and magnetic effects.

The next step is the development of a mathematical model capable of combining the internal photoelectric effect and the Hall effect in order to achieve a higher amplitude of the sensor output voltage U_H.

The planar topology proposed in this work (**Fig. 1**) enables uniform distribution of the near-surface current within the sensing element and ensures measurement stability. A key feature is that the photosensitive region of the sensor overlaps the carrier transport paths; so that even small variations in illumination lead to significant changes in carrier concentration. This creates favorable conditions for enhancing magnetic field sensitivity without the need to modify the sensor geometry.

The low temperature dependence of carrier mobility and concentration for the selected CdS sample (less

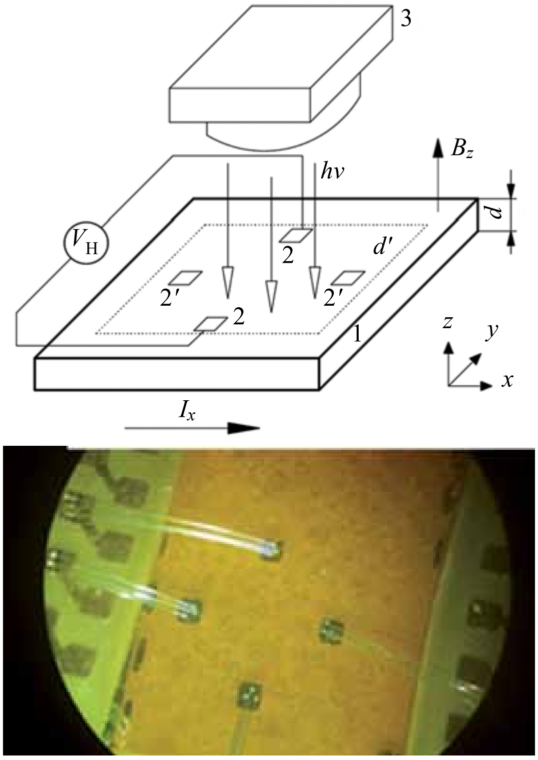

Fig. 1. Topology and external view of the proposed planar Hall sensor with a photosensitive active region:

1 — semiconductor plate; *2*, *2′* — metallic contacts on the surface of the plate; *3* — irradiation source (λ=532 nm, P=100 mW); d, d'— thickness of the sensor and the active layer, respectively (under irradiation $d' << d$); I_x — current through the sensor; B_z — magnetic flux density of the applied magnetic field; V_H — Hall voltage

ISSN 3083-6530 (Print)
ISSN 3083-6549 (Online)

than 1%/1 K) makes it possible to derive analytical relationships assuming an average temperature of $T=297\pm2$ K=const.

The number of absorbed photons is determined by the absorption coefficient α(λ), which is a function of the radiation wavelength λ. For photons with energy $h\nu\geq E_g$, charge carrier photogeneration is efficient. The carrier generation process is described by the generation rate:

$$D=\alpha\Phi, \qquad (10)$$

where Φ is photon flux (the number of photons per unit area per unit time). This parameter indicates how many electron-hole pairs are generated within a unit near-surface volume over a given time interval.

Not all generated carriers contribute to a change in electrical conductivity, since recombination processes occur. The number of carriers that effectively influence the conductivity variation is determined by the photogeneration efficiency and the average carrier lifetime τ. In particular, the steady-state excess carrier concentration can be estimated as follows:

$$\Delta n\approx D\tau. \qquad (11)$$

Higher absorption efficiency and longer carrier lifetime result in increased charge carrier photogeneration. Under optical irradiation, the number of carriers increases by Δn (electrons) or Δp (holes). Accordingly, the effective concentrations of electrons and holes, respectively, to be expressed as follows:

$$n_{\text{eff}}=n_0+\Delta n; \qquad (12)$$

$$p_{\text{eff}}=p_0+\Delta p. \qquad (13)$$

Under optical irradiation, the concept of an effective thickness of the photosensitive semiconductor, denoted as d', arises. This parameter defines the depth to which light penetrates into the material, thereby affecting charge carrier generation and, consequently, its electrical properties. According to the Beer–Lambert–Bouguer law, the light intensity decreases exponentially with the penetration depth:

$$I(z)=I_0\exp(-\alpha z), \qquad (14)$$

where I_0 is the initial radiation intensity at the surface.

The quantity inverse to the absorption coefficient (1/α) corresponds to the thickness of the semiconductor layer d' over which the light intensity decreases by a factor of e. This implies that the effective thickness of the photosensitive layer is defined as:

$$d'=1/\alpha. \qquad (15)$$

With increasing absorption coefficient, the effective thickness decreases, since light is absorbed more strongly within a shallower depth. As a result, an active region is formed (**Fig. 2**), where the effective thickness d' is smaller than the substrate thickness d. According to expression (3), this enables a higher Hall voltage to be obtained without compromising the mechanical strength of the structure.

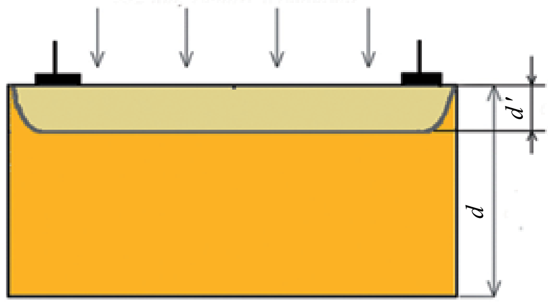

Fig. 2. Formation of the active region in a photosensitive planar Hall sensor during irradiation of a CdS substrate

The exponential decay of light intensity within the crystal thickness indicates that the effective photosensitive thickness is generally smaller than the actual sensor thickness. This parameter depends on the irradiation wavelength: short-wavelength radiation generates carriers near the surface, while long-wavelength radiation penetrates deeper into the material. Thus, the choice of the irradiation spectrum serves as a tool for controlling the spatial profile of photogeneration, enabling optimization of sensor operation under different conditions.

Equation (3) can be rewritten by taking into account expressions (12) and (13):

$$U_H=\frac{p_{eff}\mu_h^2-n_{eff}\mu_e^2}{q\left(p_{eff}\mu_h+n_{eff}\mu_e\right)^2}\frac{IB}{d}G=$$

$$=\frac{(p_0+\Delta p)\mu_h^2-(n_0+\Delta n)\mu_e^2}{q\left((p_0+\Delta p)\mu_h+(n_0+\Delta n)\mu_e\right)^2}\frac{IB}{d}G. \qquad (16)$$

If we introduce the coefficient $b=\mu_e/\mu_h$, then equation (8) can be written in the following form:

$$U_H=\frac{(p_0+\Delta p)-(n_0+\Delta n)b^2}{\left((p_0+\Delta p)+(n_0+\Delta n)b\right)^2}\frac{IB}{qd}G. \qquad (17)$$

To verify the theoretical model and to separate the unknown quantities, one may assume that the Hall sensor is irradiated with sufficiently high intensity I, such that $d=d'$. Under this irradiation regime, photogeneration becomes uniform throughout the entire crystal volume, which allows the modified value of the charge carrier concentration to be applied consistently.

For low and moderate irradiation intensities, the increase in electron and hole concentrations can be assumed to be proportional to the photon flux Φ:

$$\Delta n=\eta(\lambda)\Phi\tau_e/l_e; \qquad (18)$$

$$\Delta p=\eta(\lambda)\Phi\tau_h/l_h; \qquad (19)$$

where $\tau_{e/h}$, $l_{e/h}$ is the average lifetimes and free paths of electrons and holes, respectively.

ISSN 3083-6530 (Print)
ISSN 3083-6549 (Online)

Taking these expressions into account, equation (17) can be rewritten as follows:

$$U_H = \frac{\left(p_0 + \frac{\eta(\lambda)\Phi\tau_h}{l_h}\right) - \left(n_0 + \frac{\eta(\lambda)\Phi\tau_e}{l_e}\right)b^2}{\left(\left(p_0 + \frac{\eta(\lambda)\Phi\tau_h}{l_h}\right) + \left(n_0 + \frac{\eta(\lambda)\Phi\tau_e}{l_e}\right)b\right)^2}\frac{IB}{qd}G. \quad (20)$$

Photogeneration may, in some cases, affect charge carrier scattering, lead to the formation of additional recombination centers, and induce defects in the substrate structure. However, these effects are not considered in the present mathematical model due to their relatively weak influence. At the same time, the authors of [23] demonstrate that photogeneration can significantly modify the electrical conductivity of semiconductors, and study [24] showed that the additional generation of carriers alters the electrical transport characteristics of the material. As a result of the assumptions made and the transformations performed, a relationship can be established between the Hall voltage under illumination $U_{H,il}$ and in the dark state $U_{H,d}$:

$$\frac{U_{H,il}}{U_{H,d}} = \frac{\left(p_0 + \frac{\eta(\lambda)\Phi\tau_h}{l_h}\right) - \left(n_0 + \frac{\eta(\lambda)\Phi\tau_e}{l_e}\right)b^2}{\left(\left(p_0 + \frac{\eta(\lambda)\Phi\tau_h}{l_h}\right) + \left(n_0 + \frac{\eta(\lambda)\Phi\tau_e}{l_e}\right)b\right)^2} \times$$

$$\times \frac{(p_0 + n_0 b)^2}{p_0 - n_0 b^2}\frac{d}{\alpha}. \quad (21)$$

By substituting the representative parameters of the CdS single crystal employed in the planar Hall sensor developed in this study:
$p_0 = 10^{20}\,m^{-3}$; $n_0 = 10^{18}\,m^{-3}$; $\eta = 0.8$; $\alpha = 1.5 \cdot 10^{-3}\,m^{-1}$;
$\tau_h = 10^{-7}\,s$; $\tau_e = 10^{-8}\,s$; $b = 5$; $d = 0.5 \cdot 10^{-3}\,m$;
$\Phi = 10^{21}\,m^{-2} \cdot s^{-1}$; $l_h = 5.8 \cdot 10^{-6}\,m$; $l_e = 1.1 \cdot 10^{-6}\,m$.
The resulting theoretical ratio of the Hall voltage under illumination to that in the dark state is $U_{H,il}/U_{H,d} = 1.893$.

The modeling results presented in **Fig. 3** indicate that the increase in Hall voltage as external irradiation is not linear and exhibits a pronounced maximum. This behavior indicates the existence of an optimal combination of the active-layer thickness and photon flux at which the photogeneration of electrons and holes provides the largest increase in Hall voltage. At higher flux levels, the effect diminishes due to recombination processes. Hence, the model enables prediction of the limits of effective sensor operation and helps to avoid regimes of oversaturation and unnecessary energy consumption. The ratio $U_{H,il}/U_{H,d}$ increases as α decreases and at low values of Φ, however, with further increases in Φ it decreases, as shown in Fig. 3. The maximum is reached when Φ attains a certain low value and $\alpha = 0.2$ mm^{-1}. Nevertheless, the active semiconductor layer is formed as a result of

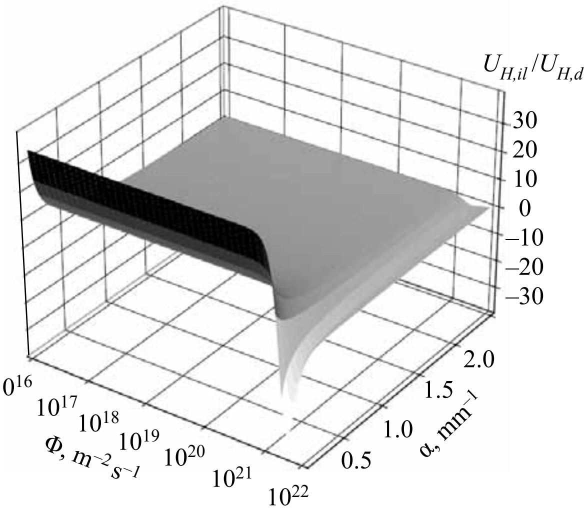

Fig. 3. Ratio of the Hall voltage under illumination to that in the dark state for CdS (a maximum value of 20 is achieved at an effective thickness of 0.2 mm, formed by a photon flux intensity of $2.6 \cdot 10^{17}$ m$^{-2} \cdot$s^{-1})

irradiation, and its thickness depends on the photon flux, quantum efficiency, irradiation wavelength, and angle of incidence at the surface.

Influence of Noise and Modeling Errors on the Calculation of the Hall Voltage

The mathematical model presented in this work accounts for charge carrier photogeneration and is based on the classical expression for the Hall voltage, with variations in charge carrier concentration included. To ensure the linearity of the model, the excess carrier concentration Δn must be much smaller than the baseline concentration n_0 (i.e., $\Delta n \ll n_0$). Under this condition, the model remains effectively linear, since small concentration perturbations do not alter the functional dependence of the Hall voltage U_H on current and magnetic field. If photogeneration becomes excessively strong ($\Delta n \approx n_0$ or $\Delta n > n_0$), the model begins to exhibit nonlinear effects, in which case even small variations in Δn may induce significant fluctuations in the output signal [25].

The photon flux Φ is one of the key parameters for controlling the Hall voltage, as high irradiation intensity may cause carrier saturation and drive the system outside the linear regime. At high quantum efficiency η(λ) even small change in irradiation intensity can result in a significant increase in the electron concentration Δn. The carrier lifetime τ, which depends on crystal quality, also affects the Hall voltage: a short lifetime leads to rapid recombination and reduces the influence of photogeneration, whereas a long lifetime enhances the effect [26]. All parameters must be chosen to ensure that the model operates within the linear range, where the assumption $\Delta n \ll n_0$ remains valid.

For the CdS/CdSe systems study [27] reports infrared quenching (IR quenching) of the photo-Hall effect in doped CdS:Cu/ZnS:Cu, materials, variations in carrier mobility as a function of photoelectron density in CdSe, as well as photoconductivity mechanisms in polycrystalline CdS involving trap states. These results directly confirm the influence of $\Delta n(\Phi, \lambda)$, τ and defects on the formation of the Hall voltage and the sensor sensitivity.

Thermal noise (also known as Johnson–Nyquist noise) is an inherent characteristic of any electrical system. It is defined as

$$v_n = \sqrt{4k_B TR\Delta f} ,$$

where k_B is Boltzmann constant;
T is absolute temperature;
R is resistance;
Δf is measurement bandwidth.

In the context of Hall sensors, thermal noise can influence both the measurement of the Hall output voltage and the overall system stability. If the noise level exceeds the signal variation induced by photogeneration, device sensitivity decreases. Therefore, appropriate design measures (e.g., low noise amplifiers and bandwidth optimization) must be implemented to mitigate the influence of thermal noise on measurements [28].

Defects and inhomogeneities in the crystal can lead to the formation of localized carrier traps, which may reduce the effective carrier lifetime τ and the value of Δn. In certain regions of the crystal, the local carrier concentration may differ from the average value n_0, resulting in a nonuniform response to irradiation. Furthermore, defects can introduce additional sources of flicker noise (1/*f* noise), thereby reducing measurement stability [29].

Experimental Investigation of the Developed Planar Hall Sensor

To eliminate thermoelectric EMF and minimize the influence of temperature-dependent carrier mobility, all Hall voltage measurements were performed at a constant temperature. The sample temperature was maintained at 297 K with an allowable deviation of no more than ±2 K. This made it possible to minimize the influence of $\mu(T)$ and $n(T)$ and to isolate the contribution of the internal photoelectric effect to the formation of the Hall voltage.

The results of the experimental investigation of the developed planar Hall sensor with a photosensitive active region are presented in **Fig. 4**. They confirm the theoretically substantiated increase in the Hall voltage under external irradiation. The measurement results show that the model describes the variation of the Hall voltage as a function of sensor parameters, irradiation, and external magnetic field with an error not exceeding 5% for currents above 40 mA. At low currents (<40 mA), a markedly larger Hall voltage is observed, arising from noise factors, charge accumulation in the diffusion capacitance of the crystal, carrier injection and drift

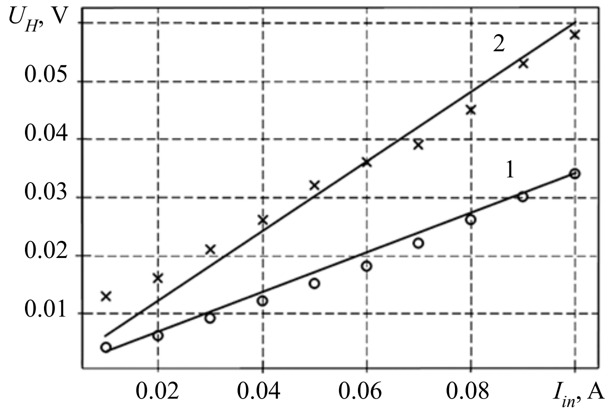

Fig. 4. Experimental (*symbols*) and theoretical (*lines*) dependences of the Hall voltage on current for CdS, obtained without irradiation (*1*) and with irradiation (*2*)

associated with edge effects, as well as the motion of photoelectrons in the near-surface region of the crystal, where resistivity decreases sharply. Under these conditions, pronounced nonlinear small-signal effects become evident.

The experimental results demonstrate an approximately 2.8-fold increase in the Hall sensor sensitivity to the magnetic field at a current of 10 mA, which significantly exceeds the prediction of the mathematical model and warrants further investigation.

Conclusions

The developed mathematical model of a planar Hall sensor enables both qualitative and quantitative evaluation of the influence of photoelectron generation on the Hall voltage in CdS-based structures. A universal approach is proposed for enhancing of magnetic field measurement sensitivity using energy-efficient photosensitive Hall sensors with low power consumption.

Experimental investigations confirmed the nearly twofold increase in the Hall voltage under irradiation of the CdS crystal predicted by the mathematical model, demonstrating good agreement between theory and experiment. The proposed planar sensor architecture opens the possibility of employing photosensitive Hall sensors in high-precision and energy-efficient measurement systems.

The mathematical model indicates that, for Hall sensors with a photosensitive active region, materials with a maximal difference between electron and hole mobilities should be selected, along with a peak spectral sensitivity in the optical or ultraviolet region to minimize the thickness of the active layer.

The next stage of research will extend the model to describe the dynamic characteristics of the sensor under modulated light intensity conditions, as well as accounting for the effects of temperature and crystal structure defects in low-power operating regimes, i.e., developing a small-signal model of the planar Hall sensor.

ISSN 3083-6530 (Print)
ISSN 3083-6549 (Online)

REFERENCES

[1] S. M. Sze, *Physics of Semiconductor Devices*, 3rd ed. Hoboken, NJ, USA: Wiley, 2006.

[2] M. J. Caruso, C. H. Smith, T. Bratland, and R. Schneider, “A new perspective on magnetic field sensing,” *Sensors*, vol. 17, no. 9, pp. 258–264, 2000. Available: https://surl.li/yyvpuk

[3] W. Bolton, *Sensors and Actuators: Engineering System Instrumentation*, 2nd ed. Oxford, U.K.: Newnes, 2021.

[4] L. Liu, X. Guo, W. Liu, and C. Lee, “Recent progress in the energy harvesting technology—From self-powered sensors to self-sustained IoT, and new applications,” *Nanomaterials*, vol. 11, no. 11, Art. no. 2975, 2021, doi: 10.3390/nano11112975.

[5] A. Musiienko, R. Grill, P. Moravec, P. Fochuk, I. Vasylchenko, H. Elhadidy, et al., “Photo-Hall-effect spectroscopy with enhanced illumination in p-$Cd_{1-x}Mn_xTe$ showing negative differential photoconductivity,” *Phys. Rev. Applied*, vol. 10, pp. 014019, 2018, doi: 10.1103/PhysRevApplied.10.014019

[6] S. E. Schacham, and E. Finkman, “Light-modulated Hall effect for extending characterization of semiconductor materials,” *J. Appl. Phys*., vol. 60, pp. 2860–2865, 1986, doi: 10.1063/1.337070

[7] A. I. Galuza and A. B. Beznosov, “Optical functions of the Drude model: transformation of the spectra over wide ranges of parameters,” *Low Temp. Phys*., vol. 27, pp. 216–227, 2001, doi: 10.1063/1.1355519

[8] N. J. Gantzler, “An alternative approach to the extended Drude model,” *J. Appl. Spectrosc*., vol. 85, pp. 361–364, 2018, doi: 10.1007/s10812-018-0657-x

[9] I. V. Maznichenko, “Tunable 2D electron gas at the $LaAlO_3$/$SrTiO_3$(001) interface,” *Phys. Rev. Materials*, vol. 3, pp. 074006, 2019, doi: 10.1103/PhysRevMaterials.3.074006

[10] J. H. Davies, “The two-dimensional electron gas,” in *The Physics of Low-Dimensional Semiconductors: An Introduction,* Cambridge: Cambridge University Press, 1997, pp. 329–370, doi: 10.1017/CBO9780511819070.011

[11] P. Ritzinger, and K. Vyborny, “Anisotropic magnetoresistance: materials, models and applications,” *R. Soc. Open Sci*., vol. 10, iss. 10, 2023, doi: 10.1098/rsos.230564

[12] C.-J. Zhao, “Research progress in anisotropic magnetoresistance,” *Rare Metals*, vol. 32, pp. 213–224, 2013, doi: 10.1007/s12598-013-0090-5

[13] B. G. Streetman, and S. Banerjee, *Solid State Electronic Devices*, 6th ed. Upper Saddle River, NJ, USA: Prentice Hall, 2006.

[14] V. Bruevich, H. H. Choi, and V. Podzorov, “The photo-Hall effect in high-mobility organic semiconductors,” *Adv. Funct. Mater*., vol. 31, pp. 2006178, 2021, doi: 10.1002/adfm.202006178

[15] Y. Chen, H. T. Yi, and V. Podzorov, “High-resolution ac measurements of the Hall effect in organic field-effect transistors,” *Phys. Rev. Applied*, vol. 5, pp. 034008, 2016, doi: 10.1103/PhysRevApplied.5.034008

[16] M. Schubert, P. Kühne, V. Darakchieva, and T. Hofmann, “Optical Hall effect model description: tutorial,” *J. Opt. Soc. Am*. A, vol. 33, pp. 1553–1568, 2016, doi: 10.1364/JOSAA.33.001553

[17] C. Jacoboni, and L. Reggiani, “The Monte Carlo method for the solution of charge transport in semiconductors with applications to covalent materials,” *Rev. Mod. Phys.*, vol. 55, no. 3, pp. 645–705, 1983, doi: 10.1103/RevModPhys.55.645

[18] Y. Tsividis, and C. McAndrew, *Operation and Modeling of the MOS Transistor*, 3rd ed. Oxford, U.K.: Oxford Univ. Press, 2011.

[19] R. S. Popovic, *Hall Effect Devices: Magnetic Sensors and Characterization of Semiconductors*. Bristol, U.K.: Institute of Physics Publishing, 2004.

[20] R. F. Pierret, *Semiconductor Device Fundamentals*. Reading, MA, USA: Addison Wesley, 1996.

[21] M. Razeghi, and R. Baker, *Modern Semiconductor Device Physics*. San Diego, CA, USA: Academic Press, 2007.

[22] J. Singh, *Semiconductor Optoelectronics: Physics and Technology*. New York, NY, USA: McGraw-Hill, 2003.

[23] P. Y. Yu, and M. Cardona, *Fundamentals of Semiconductors: Physics and Materials Properties*, 4th ed. Berlin, Germany: Springer, 2010, doi: 10.1007/978-3-642-00710-1

[24] J. I. Pankove, *Optical Processes in Semiconductors*. New York, NY, USA: Dover Publications, 1971.

[25] D. K. Ferry, and S. M. Goodnick, *Transport in Nanostructures*. Cambridge, U.K.: Cambridge Univ. Press, 1997, doi: 10.1017/CBO9780511626128

[26] R. A. Smith. *Semiconductor Fundamentals*. Oxford University Press, 2014.

[27] B. Ch. Burgett, and C. Ch. Lin, “Infrared quenching of the luminescence and photo-hall effect of ZnS:Cu and CdS:Cu crystals”, *Journal of Physics and Chemistry of Solids*, vol. 31, iss. 6, 1970, pp. 1353–1359, doi: 10.1016/0022-3697(70)90139-3.

[28] J. H. Davies, *The Physics of Low-Dimensional Semiconductors: An Introduction*. Cambridge University Press, 1998.

[29] B. K. Ridley, *Quantum Processes in Semiconductors* (5th ed.). Oxford University Press, 2013.

Received 01.09 2025

DOI: 10.15222/TKEA2025.3-4.15
УДК 681.586.728

Віктор СЕРГІЙЧУК, Остап ОЛІЙНИК

Україна, м. Київ, КПІ імені Ігоря Сікорського

E-mail: ostap.oliinyk@gmail.com

РОЗРОБКА МАТЕМАТИЧНОЇ МОДЕЛІ ФОТОЧУТЛИВОГО СЕНСОРА ХОЛЛА НА ОСНОВІ CdS

Запропоновано математичну модель фоточутливого сенсора Холла виготовленого на основі монокристалу CdS, в якому використовується внутрішній фотоефект. Математична модель описує зміну концентрації та рухливості носіїв зарядів під дією опромінення й дозволяє оцінити приріст чутливості сенсора до магнітного поля завдяки зміні параметрів матеріалу сенсора. Теоретично встановлено і підтверджено експериментально, що при зовнішньому опроміненні активної області сенсора напруга Холла збільшується двократно. Розроблений підхід може бути використаний для оптимізації планарних сенсорів у системах, які потребують високої точності, чутливості та енергоефективності.

Ключові слова: ефект Холла, фоточутливий сенсор Холла, CdS, математичне моделювання, планарний сенсор Холла.